Pion optical potential with Δ dynamics

B. Karaoglu
Istanbul Teknik Universitesi, Maslak, Istanbul, Turkey

E. J. Moniz
Center for Theoretical Physics, Department of Physics and Laboratory for Nuclear Science, Massachusetts Institute of Technology, Cambridge, Massachusetts 02139
(Received 1 July 1985)

A pion optical potential is constructed which incorporates the Δ dynamics found to be important in Δ-hole analyses of pion scattering from light nuclei. These dynamics include Δ propagation, binding and Pauli blocking, and a Δ spreading potential. We employ a local density approximation for the medium-modified Δ propagator, resulting in a computationally flexible tool for the analysis of pion-nucleus data. We reproduce the Δ-hole results for π-^{16}O scattering satisfactorily. Elastic $\pi^{\pm}$-^{208}Pb scattering is described very well with the same strongly damping spreading potential found for light nuclei. The pion wave functions in the medium are substantially modified by the Δ dynamics.

I. INTRODUCTION

Pion-nucleus interactions have been studied intensively over the last decade in the energy regime corresponding to Δ excitation. A prime motivation for these studies has been the attempt to learn about Δ dynamics in the nuclear medium. A series of quantitative theoretical studies[1–4] carried out within the Δ-hole formulation of pion-nucleus scattering has had considerable success in reproducing and correlating data for *s*- and *p*-shell nuclei with a rather compact mean field characterization of the Δ-nucleus interaction. Strong damping of Δ motion in nuclei is indicated. Although no satisfactory microscopic theory exists, the origin of this damping clearly lies in the annihilation process[5] $\Delta N \rightarrow NN$, which is a basic reaction for understanding the role of subnucleonic degrees of freedom in the strong interaction. The Δ-hole studies pointed out clearly that careful treatment of the rather uninteresting dynamics associated with resonance propagation, nuclear binding, and Pauli blocking is essential for extracting information on the Δ-nucleus interaction. Unfortunately, microscopic treatment of these effects is computationally nontrivial so that, on one hand, standard optical potential treatments[6,7] (based upon the static approximation) do not adequately incorporate this physics while, on the other hand, the Δ-hole calculations (which have incorporated it) have been restricted to light nuclei. The goal of the work presented here is construction of a pion optical potential which builds in Δ dynamics while still being computationally flexible. Our approach is based upon local density approximation to the Δ propagator, with the important medium corrections guided by the available Δ-hole results. With this optical potential, we study the Δ-nucleus interaction in elastic $\pi^{\pm}$ ^{208}Pb scattering. The result is a reinforcement of the mean field characterization developed in the analyses of light systems.

Nuclear structure studies have provided another important motivation for the study of intermediate energy pion-nucleus scattering, particularly through exploitation of the isospin structure of the Δ-dominated πN amplitude. For example, comparisons of π^+ and π^- scattering have been employed to study neutron distributions in elastic scattering and isospin mixing of particle-hole states in inelastic scattering.[8] The static optical potentials alluded to above[6,7] generally are used in the analyses, but it is known that the Δ-nucleus dynamics are important for quantitative analysis.[9,10] Consequently, we feel that the optical potential described below, by incorporating the Δ dynamics in a manner which allows simple use and efficient computation, can be a valuable tool for the analysis of pion-nucleus data.

In Sec. II, we review the Δ-hole formalism briefly and present our construction of the optical potential. The Δ kinetic energy, binding, and Pauli blocking effects mentioned earlier are included as modifications of the Δ propagator in the nucleus. These effects are part of the first order optical potential (i.e., occur at the one-hole level), but are generally ignored or reduced to a simple parameter change in standard static treatments. The Δ-hole calculations[1–4] dictate a more refined treatment. We follow the Δ-hole approach and incorporate higher order effects through a Δ spreading potential which damps Δ propagation in the medium. Clearly, this approach is most appropriate for isolating the physics of Δ-nucleus interactions. Further, we note that this approach leads to a phenomenology very different from that enfored through phenomenological parametrization of a second-order pion optical potential. This is seen easily with a schematic representation of the optical potential. The first order optical potential has the structure

$$V^{(1)}=\rho\frac{C}{E-E_R+i\Gamma/2}\ , \tag{1}$$

where the Breit-Wigner denominator characterizes the Δ and ρ is the nuclear density. With a Δ damping width proportional to the density, the optical potential becomes

$$V=\rho\frac{C}{E-\tilde{E}_R+\frac{i}{2}(\Gamma+\Gamma_A\rho/\rho_0)}\ , \tag{2a}$$

$$\mathrm{Im}\,V=-\rho\frac{\frac{C}{2}(\Gamma+\Gamma_A\rho/\rho_0)}{(E-\tilde{E}_R)^2+\frac{1}{4}(\Gamma+\Gamma_A\rho/\rho_0)^2}\ . \tag{2b}$$

As can be seen from Eq. (2a), the additional Δ damping in the medium decreases pion optical absorption at resonance, while standard parametrizations

$$V\equiv V^{(1)}+V^{(2)} \tag{3}$$

would lead to increased absorption (unless $\mathrm{Im}V^{(2)}$ has the "wrong" sign). The basic problem with Eq. (3) lies in the failure to incorporate the shadowing of the annihilation process on the in-medium elastic πN amplitude. This effect is explicit in Eq. (2b). The importance of this effect will be seen in a substantially enhanced pion density in the nucleus at resonance energy upon inclusion of the Δ-nucleus dynamics. Since we envision applications to heavy nuclei, the isospin dependence of the spreading potential found to be important for quasielastic reactions[11] is included.

Section III contains our calculated results and comparisons with data. We first present a fairly detailed comparison with π^+-^{16}O elastic data and with the Δ-hole results. The latter comparison is particularly important in that the Δ-hole calculations provide a standard against which our local density approximation can be tested. We stress that the local density approximation is applied to the Δ propagator, which is short-ranged because of the $\Delta\rightarrow\pi$N decay process. The comparisons are satisfactory and we proceed to a comparison with $\pi^{\pm}$-^{208}Pb elastic data. The spreading potential extracted from analyses of p-shell nuclei leads to acceptable comparisons with the data. We then discuss the properties of the pion scattering wave function, which is a central input to calculations of inelastic processes. We present one application, namely, a calculation of coherent π^0 photoproduction, demonstrating the importance of a dynamical treatment of the production operator in a distorted wave calculation. A few concluding remarks are offered in Sec. IV.

II. CONSTRUCTION OF THE PION OPTICAL POTENTIAL

A. The Δ-hole model

The dominance of intermediate energy pion-nucleon scattering by Δ excitation leads naturally to a description of pion-nucleus scattering which focuses upon Δ propagation in the medium. The picture is that the incoming pion (or photon) excites a Δ-hole configuration and that the final states in elastic or inelastic scattering are reached from such configurations. The intermediate Δ-hole propagator contains the physics. The focus on the Δ, rather than the pion, degree of freedom not only provides a convenient framework for isolating the Δ-nucleus interaction effects but also for implementing the "first order" dynamics discussed in the Introduction.

The structure of the Δ-hole model[12] for pion elastic scattering can be given in the projection operator formalism. P_0 projects onto the elastic channel, while P_1 denotes the space of pion-plus-one-particle-hole states. The Δ-hole configurations are in the D space, and are assumed to act as doorways from the elastic channel into all more complicated configurations (the nonresonant πN interactions will be discussed later). The Q space is the remainder, consisting of pion-plus-multi-particle-hole states and of annihilation channels, which contain neither a pion nor a Δ. The coupled-channel Lippmann-Schwinger (LS) equations then yield the simple form for the elastic transition matrix

$$T_{P_0P_0}=V_{P_0D}G_{\Delta h}V_{DP_0}\ , \tag{4}$$

where V_{P_0D} is the πN-Δ transition operator and $G_{\Delta h}$ designates the medium-modified Δ-hole propagator,

$$G_{\Delta h}=(E-H_\Delta-\tilde{V}_{DP_1}G_{P_1}\tilde{V}_{P_1D}-V_{DP_0}G^0_{P_0}V_{P_0D}-V_{DQ}G_QV_{QD})^{-1}\ , \tag{5}$$

with

$$G^0_{P_0}=(E^+-H_{P_0P_0})^{-1}\ , \tag{6a}$$

$$G_{P_1}=(E^+-H^0_{P_1P_1}-V_{P_1Q}G_QV_{QP_1})^{-1}\ , \tag{6b}$$

$$G_Q=(E^+-H^0_{QQ}-V_{QQ})^{-1}\ , \tag{6c}$$

$$H_{P_0P_0}=T_\pi+H^{\mathrm{SM}}_A\ , \tag{7a}$$

$$H_\Delta=M_\Delta+T_\Delta+V_\Delta+H^{\mathrm{SM}}_{A-1}\ , \tag{7b}$$

$$\tilde{V}_{P_1D}=V_{P_1D}+V_{P_1Q}G_QV_{QD}\ . \tag{8}$$

The term with $\tilde{V}_{P_1D}$ in Eq. (5) builds up the free Δ self-energy except for the Pauli-blocked states. The term with V_{DP_0} is the pion elastic rescattering term and V_{QD} designates the more complicated coupling to multi-particle-hole states. The binding potential V_Δ is taken to be the same as that for nucleons. The term with $\tilde{V}_{P_1D}$ is combined with H_Δ to make explicit the free resonant propagator, the Pauli self-energy, and part of the Q-space coupling,

$$\begin{aligned}E-H_\Delta-\tilde{V}_{DP_1}G_{P_1}\tilde{V}_{P_1D}&=E-H_\Delta-V_{DP_1}G^0_{P_1}V_{P_1D}-\Sigma'_Q\\&=E-H_\Delta-[\Sigma_{\mathrm{free}}(E-H_\Delta)\\&\qquad+\Sigma_{\mathrm{Pauli}}]-\Sigma'_Q\\&=D(E-H_\Delta)-\Sigma_{\mathrm{Pauli}}-\Sigma'_Q\ ,\end{aligned} \tag{9}$$

where

$$D(E)=E-M_\Delta-\Sigma_{\mathrm{free}}(E)\equiv E-E_R(E)+i\frac{\Gamma(E)}{2} \tag{10}$$

is the inverse of the free-space dressed Δ propagator in the Δ rest frame. The terms with V_{DQ} and Σ'_Q are then combined into a phenomenological spreading potential Σ_{spr}, so that the Δ-hole propagator is finally written as

$$G_{\Delta h}(E)=[D(E-H_\Delta)-W(E)-\Sigma_{\text{Pauli}}(E)-\Sigma_{\text{spr}}(E)]^{-1}, \quad W(E)=V_{DP_0}G^0_{P_0}V_{P_0D}\ . \tag{11}$$

The elastic pion amplitude is then given as an expectation value in Δ-hole doorway states,

$$\langle \mathbf{k}';0\,|\,T_{P_0P_0}(E)\,|\,\mathbf{k};0\rangle = (N_{\mathbf{k}}N_{\mathbf{k}'})^{-1}\langle D_0(\mathbf{k}')\,|\,G_{\Delta h}(E)\,|\,D_0(\mathbf{k})\rangle\ , \tag{12}$$

$$|\,D_0(\mathbf{k})\rangle \equiv N_{\mathbf{k}}V_{DP_0}\,|\,\mathbf{k};0\rangle\ , \tag{13}$$

$$\langle D_0(\mathbf{k})\,|\,D_0(\mathbf{k})\rangle \equiv 1\ .$$

Calculations proceed by taking the partial wave decomposition of the doorway states and evaluating the matrix elements in Eq. (12) within a shell model (SM) basis. All of the terms in Eq. (11) except for Σ_{spr} are evaluated microscopically. As discussed below, the shape of the spreading potential is fixed and the strength parameters determined by the data. The binding and propagation effects contained in H_Δ show a strong L dependence, in contrast to the assumption made in static approximations. The Pauli term substantially reduces the $\Delta\rightarrow\pi$N decay width in the medium. The elastic rescattering term W is very large, because of the strong optical absorption of pions. This term will not be present in the optical potential; instead, this physics is built in by iteration of V_{opt} in the pion-nucleus elastic channel Lippmann-Schwinger equation. Finally, the spreading potential is found to damp the Δ strongly in studies of light nuclei.[1–4] We shall extend the analysis to heavy nuclei in the next section.

B. The optical potential

We now develop a momentum space optical potential based on the isobar dynamics. Its formal expression is similar to that for the T-matrix Eqs. (11)—(13), with the rescattering term W deleted. In order to include the important Coulomb interaction, diagonal terms are added on various subspaces. The optical potential has the form

$$U(\mathbf{k}',\mathbf{k})=U_B+\langle \mathbf{k};0\,|\,V_{P_0D}[D(E-H_\Delta)-\Sigma_{\text{Pauli}}-\Sigma_{\text{spr}}(E)]^{-1}V_{DP_0}\,|\,\mathbf{k};0\rangle \equiv U_B+U_\Delta\ . \tag{14}$$

The background potential U_B includes both nonresonant pion-nucleon interactions and the pion Coulomb interaction. The first order static treatment of the nonresonant terms is taken directly from the optical potential PIPIT.[6] We also include a phenomenological local S-wave potential

$$U_B^S(r)=B_0[\rho(r)/\rho(0)]^2\ . \tag{15}$$

A repulsive potential of this form, the origin of which is not understood, has been found to be important for scattering below 100 MeV. In comparing with data, we have taken $B_0=12$ MeV. The Δ Hamiltonian includes a Coulomb term in addition to the binding potential, the latter taken to have a depth of 55 MeV (any error here will show up as a modification of the phenomenological central spreading potential).

Equation (14) presents a calculational problem as complex as that offered by the full Δ-hole calculations. Rather than attempting to diagonalize $G_{\Delta h}$, we calculate with a Δ propagator in the local density approximation. As stated earlier, this approximation will be tested in ^{16}O and should be at least as good for heavy nuclei where the propagation distance of a free Δ (<1 fm) is small compared to nuclear density variation parameters. With this approximation and using the eigenstates of a shell-model Hamiltonian for nucleons, we have

$$U_\Delta^\lambda(\mathbf{k}',\mathbf{k})=\langle \mathbf{k}',\lambda;0\,|\,U_{P_0P_0}\,|\,\mathbf{k},\lambda;0\rangle = \sum_{\substack{\mathrm{N}\\(\mathrm{occ})}}\int\int \frac{d\mathbf{p}}{(2\pi)^3}\frac{d\mathbf{p}'}{(2\pi)^3}\psi^*_{\mathrm{N}}(\mathbf{p}')\frac{G}{M_{\mathrm{N}}}h(K'^2)\mathbf{K}'\cdot\mathbf{S}^+T^{\lambda+}\langle N^{-1}\,|\,G_\Delta(\mathbf{p}'+\mathbf{k}',\mathbf{p}+\mathbf{k};E)\,|\,N^{-1}\rangle \times\frac{G}{M_{\mathrm{N}}}h(K^2)\mathbf{K}\cdot\mathbf{S}T^\lambda\psi_{\mathrm{N}}(\mathbf{p})\ , \tag{16}$$

where $\mathbf{k}$ and $\mathbf{k}'$ designate the initial and final pion momenta in the pion-nucleus c.m. system, $\mathbf{K}$ and $\mathbf{K}'$ are the relative π-N momenta, and λ is the pion charge index. The $\pi\mathrm{N}\rightarrow\Delta$ transition operator V_{DP_0} has the form

$$V_{DP_0}=\frac{G}{M_{\mathrm{N}}}h(K^2)\mathbf{K}\cdot\mathbf{S}T^\lambda\ , \tag{17}$$

with the coupling constant G and a vertex function of the form

$$h(K^2)=[1+(K/\alpha)^2]^{-1}\ . \tag{18}$$

$\mathbf{S}$ and T^λ are the spin and isospin transition operators to the isobar state. The coupling constant and the cutoff parameter α were fixed by a fit to the experimental πN(3,3) phase shifts over the intermediate energy range. The values used in this work are $G^2=421$ and $\alpha=294$ MeV/c (see Ref. 14 for details of the procedure). The Δ-hole propagator is

$$G_\Delta(\mathbf{P}',\mathbf{P};E)=(2\pi)^3\delta^3(\mathbf{P}'-\mathbf{P})\{D[E-H_\Delta(\rho)]-\Sigma_{\text{Pauli}}(E,\rho)-\Sigma_{\text{spr}}(E,\rho)\}^{-1}\ , \tag{19}$$

where ρ is the local nuclear matter density. As in the Δ-hole calculations, the resonance denominator is linearized in H_Δ,

$$D(E-H_\Delta)\simeq D(E)-\gamma(E)H_\Delta\ , \tag{20}$$

$$\gamma(E)=\frac{\partial D(E)}{\partial E}\ , \tag{21}$$

$$H_\Delta=\frac{(\mathbf{p}+\mathbf{k})^2}{2M_\Delta}+V_\Delta(\rho)+V_\Delta^C(\rho)+\epsilon_j\ , \tag{22}$$

where ϵ_j is the hole energy. The relative momenta $\mathbf{K}$ and $\mathbf{K}'$ are approximated in the vertex functions only as

$$\begin{aligned}\mathbf{K}&=(M\mathbf{k}-\omega_k\mathbf{p})/(M+\omega_k)\\&\approx\mathbf{M}k/(M+\omega_k)\ ,\end{aligned} \tag{23}$$

with $\omega_k=[m_\pi^2+k^2]^{1/2}$. Writing the nucleon wave functions as

$$\psi_j(\mathbf{p})=\phi_j(\mathbf{p})\,|\,\tfrac{1}{2}\sigma_j\rangle\,|\,\tfrac{1}{2}\tau_j\rangle\ , \tag{24}$$

we obtain for a closed-shell nucleus

$$U_\Delta^\lambda(\mathbf{k}',\mathbf{k})=C(\mathbf{k},\mathbf{k}')\sum_{\mathrm{N=p,n}}(1+\lambda\tau_{\mathrm{N}})\sum_{\substack{j\\ \text{occ}}}\int d\mathbf{r}\,d\mathbf{r}'\phi_j^*(\mathbf{r}')e^{-i\mathbf{k}'\cdot\mathbf{r}'}\frac{e^{iK_\Delta(\rho)\,|\,\mathbf{r}-\mathbf{r}'\,|}}{|\,\mathbf{r}-\mathbf{r}'\,|}\phi_j(\mathbf{r})e^{i\mathbf{k}\cdot\mathbf{r}}\ , \tag{25}$$

where $\tau_{\mathrm{N}}=+\frac{1}{2}\ (-\frac{1}{2})$ for protons (neutrons) and

$$C(\mathbf{k},\mathbf{k}')=-\frac{8}{9}\left[\frac{G}{M_{\mathrm{N}}}\right]^2\frac{M_\Delta}{2\pi\gamma(E)}\mathbf{K}\cdot\mathbf{K}'h(K^2)h(K'^2)\ , \tag{26}$$

with a complex wave number for the isobar

$$K_\Delta^2(\rho)=\frac{2M_\Delta}{\gamma(E)}\left\{E-E_r+i\frac{\Gamma}{2}-\Sigma_{\text{Pauli}}(E,\rho)-\Sigma_{\text{spr}}(E,\rho)-\gamma[\epsilon_j+V_\Delta(\rho)+V_\Delta^C(\rho)]\right\}. \tag{27}$$

The optical potential has all the density dependent terms confined to the isobar propagator. Considering that the isobar propagates from $\mathbf{r}$ to $\mathbf{r}'$, the local density approximation is most naturally introduced by writing

$$\rho=\rho\left[\frac{\mathbf{r}+\mathbf{r}'}{2}\right]. \tag{28}$$

The density dependence of the various medium corrections will be discussed later.

Were it not for the dependence of K_Δ on the hole energy, the summation in Eq. (25) could be performed to give the nuclear density matrix. However, the propagator is cut off rapidly in $|\,\mathbf{r}-\mathbf{r}'\,|$ so that the variation in hole energies around a mean can be approximated. Consequently, we linearize about the weighted average of occupied energy levels,

$$\bar{\epsilon}=\frac{1}{A/4}\sum_{\substack{j\\ \text{occ}}}\epsilon_j\ , \tag{29}$$

$$K_\Delta=[\bar{K}_\Delta^2+2M_\Delta(\bar{\epsilon}-\epsilon_j)]^{1/2}\approx\bar{K}_\Delta+\frac{M_\Delta}{\bar{K}_\Delta}(\bar{\epsilon}-\epsilon_j)\ , \tag{30}$$

$$e^{iK_\Delta\,|\,\mathbf{r}-\mathbf{r}'\,|}\approx e^{i\bar{K}_\Delta\,|\,\mathbf{r}-\mathbf{r}'\,|}\left[1+i\frac{M_\Delta}{\bar{K}_\Delta}(\bar{\epsilon}-\epsilon_j)\,|\,\mathbf{r}-\mathbf{r}'\,|\right]. \tag{31}$$

This approximation is found to be very accurate throughout the resonance region. We can now perform the summation over nucleon states. We have two kinds of terms

$$\sum_{\substack{j\\ \text{occ}}}\phi_j^*(\mathbf{r}')\phi_j(\mathbf{r})=\tfrac{1}{2}\rho(\mathbf{r},\mathbf{r}') \tag{32}$$

and

$$\sum_{\substack{j\\ \text{occ}}}\epsilon_j\phi_j^*(\mathbf{r}')\phi_j(\mathbf{r})=-\tfrac{1}{4}[H(\mathbf{r})+H(\mathbf{r}')]\rho(\mathbf{r},\mathbf{r}')\ , \tag{33}$$

where $H(\mathbf{r})$ is the single-particle Hamiltonian

$$H(\mathbf{r})=-\frac{1}{2M_{\mathrm{N}}}\nabla_r^2+V_{\mathrm{N}}(r) \tag{34}$$

and $\rho(\mathbf{r},\mathbf{r}')$ is the single-particle density matrix. It has a convenient local density approximation[13]

$$\rho(\mathbf{r},\mathbf{r}')=\rho(R)\hat{j}_1(k_F(R)s)\ , \tag{35}$$

with

$$\begin{aligned}&2\mathbf{R}=\mathbf{r}+\mathbf{r}',\quad \mathbf{s}=\mathbf{r}-\mathbf{r}'\ ,\\&\hat{j}_1(x)=\frac{3}{x}j_1(x)\ ,\end{aligned} \tag{36}$$

$$k_F^3(R)=\frac{3\pi^2}{2}\rho(R)\ . \tag{37}$$

The form given by Eq. (35) is known to be good for medium and heavy nuclei and for $S\lesssim 1$ fm. It is in the same spirit as the approximations we have made so far.

After a last partial wave reduction, we write the final result as

$$U_\Delta(\mathbf{k}',\mathbf{k};E)=\frac{2}{\pi}(2\pi)^3 2\omega_K \sum_{LM} V_L^\Delta(k',k;E)Y_{LM}^*(\hat{\mathbf{k}}')Y_{LM}(\hat{\mathbf{k}}) , \tag{38}$$

$$V_L^\Delta(k',k;E)=\tilde{C}(k',k)\sum_N (1+\lambda\tau_N)\int_0^\infty dR\,R^2\int_0^\infty ds\,s^2\frac{e^{i\bar{K}_\Delta(R)s}}{s}\left\{1+\frac{iM_\Delta s}{\bar{K}_\Delta(R)}[\bar{\epsilon}+H_N(R,s)]\right\}\rho_N(R)\hat{j}_1(k_F(R)s)$$
$$\times\int_{-1}^{+1} d\mu\,\mu P_L(\mu)j_0(qR)j_0(Ps) , \tag{39}$$

$$\tilde{C}(k',k)=-\frac{2}{9}\frac{M_\Delta}{\gamma(E)\omega_k}\frac{G^2}{M_N^2}KK'h(K^2)h(K'^2) , \tag{40a}$$

$$P=\tfrac{1}{2}|\mathbf{k}+\mathbf{k}'| ,\quad q=|\mathbf{k}-\mathbf{k}'| ,\quad \mu=\hat{k}\cdot\hat{k}' , \tag{40b}$$

$$H_N(R,S)=-\frac{1}{2M_N}\nabla_S^2-\frac{1}{8M_N}\nabla_R^2+V[(R^2+\tfrac{1}{4}S^2)^{1/2}] . \tag{41}$$

In writing $H_N(R,s)$, an approximation has been made to the potential which is exact for an oscillator and very accurate for a Woods-Saxon shape. Equations (38)—(41) are the main results to be used in numerical calculations. For $N\neq Z$ nuclei, both $\bar{K}_\Delta(R)$ and $k_F(R)$ in Eq. (39) depend upon the nucleon label N=p,n in a manner defined below.

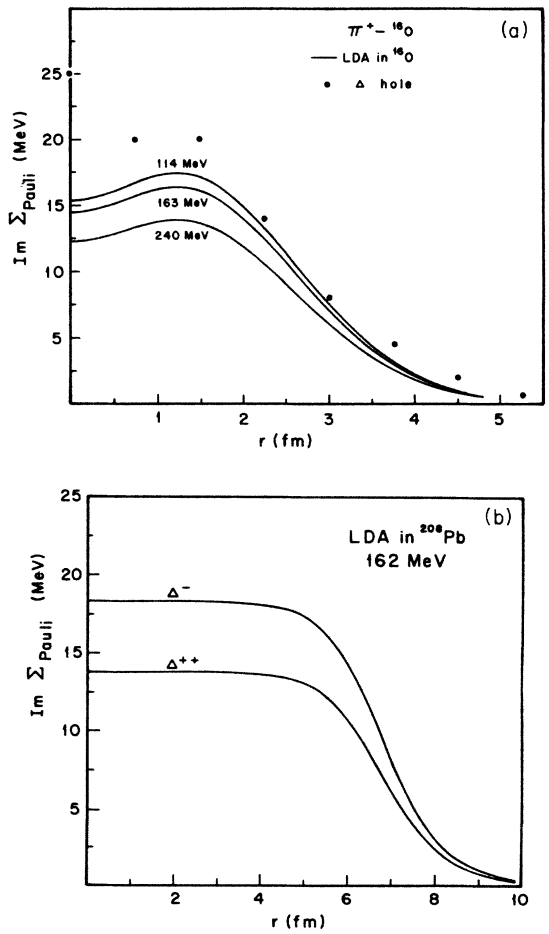

FIG. 1. Imaginary part of the Pauli self-energy using a local density for k_f. (a) ^{16}O at 114, 163, and 240 MeV. The circles represent Δ-h values of Ref. 1 for 163 MeV plotted at $r=L/k$. (b) ^{208}Pb at 162 MeV for Δ^{++} and Δ^-.

We employ the PIPIT code to solve the momentum-space Schrödinger equation. We now discuss the form of the Δ self-energy corrections to be used in Eq. (27).

1. *Pauli-blocking effect*

There is a substantial reduction of the free Δ width in nuclei, as the intermediate decay will be partly blocked by the nucleons in occupied states. The microscopic calculation of this effect in a finite nucleus is rather complicated. Instead, we use a nuclear matter calculation[14] which is fairly simple and suitable for use in a local density approximation to the Δ propagator.

With a Δ free-space self-energy given by

$$\Sigma_0(E)=G^2\frac{M_N}{E}\int\frac{d\mathbf{q}}{(2\pi)^3}\frac{q^2h^2(q^2)}{K^2-q^2+i\eta} ,$$
$$K^2=\frac{M_N}{E}[(E-M_N)^2-m_\pi^2] , \tag{42}$$

the Pauli correction is determined by restricting the integral to intermediate nucleon states above the Fermi level. Following Ref. 14, the result for a spin-saturated nucleus is

$$\Sigma_{\text{Pauli}}(E)=-G^2\frac{\alpha^4M_N}{4\pi^2E}[2\theta(k_F-\beta)W_0(k_F-\beta,0)$$
$$+W_0(k_F+\beta,|k_F-\beta|)$$
$$-W_1(k_F+\beta,|k_F-\beta|)] ,$$
$$W_n(B,A)=\int_A^B dq\,q^4\frac{h^2(q^2)}{K^2-q^2+i\eta}\left[\frac{\beta^2+q^2-k_F^2}{2\beta q}\right]^n , \tag{43}$$
$$\boldsymbol{\beta}=\frac{M_N}{E}\mathbf{p} ,$$

where $\mathbf{P}$ is the Δ momentum. Analytic expressions for the W_n are given in Ref. 14. The imaginary part of Σ_{Pauli} is shown in Fig. 1(a) for ^{16}O using a local density approximation for k_F. The free half-width is reduced by typically 30% in the nuclear interior. The real part of Σ_{Pauli}

shifts the resonance energy upward by several MeV. For comparison with the Δ-hole results, we show the partial wave doorway state expectation values for the Pauli-blocking term obtained in the Δ-hole model,[1,4] with the r dependence obtained by the crude association $kr \sim L$. The local density approximation is clearly quite reasonable for the peripheral and semiperipheral partial waves; the $L=0$ partial wave in ^{16}O has substantially more blocking than is given by the local density expression.

For application to heavy nuclei, where $N \neq Z$, we define separate neutron and proton Fermi momenta according to the local density. The local density approximation to the Pauli reduction of Δ^{++} and Δ^{-} widths in ^{208}Pb is shown in Fig. 1(b). The Δ^{++} has a width ~ 10 MeV greater in the center of the nucleus.

2. *Delta spreading interaction*

In the isobar-hole language, the spreading interaction arises from coupling to multi-particle-hole states and, in particular, to states reached by pion absorption via the mechanism $\pi NN \rightarrow \Delta N \rightarrow NN$. The very large pion absorption cross sections observed in the resonance region indicate the importance of this additional damping mechanism. The microscopic calculation of such Q-space couplings being too complicated, one uses a phenomenological spreading potential which is local and dependent on nuclear density,

$$\Sigma^{C}_{\rm spr}(E,r) = V_C \frac{\rho(r)}{\rho(0)} \ . \tag{44}$$

Through a fit to total and total elastic cross sections, Δ-h calculations of π-^{16}O scattering give

$$V_C = (20-42i) \text{ MeV} \ . \tag{45}$$

For applications to $N \neq Z$ nuclei, a model for the isospin dependence of the spreading potential is required. A simple model can be formulated by assuming the dominance of pion annihilation as the leading Q-space process. As the annihilation takes place preferentially on isoscalar n-p pairs, a reasonable isospin dependence is given by

$$(\Sigma^{C}_{\rm spr})_{\tau_N} = V_C \left[\frac{2\rho_{-\tau_N}(r)}{\rho(0)} \right] , \tag{46}$$

where τ_N is the isospin index for the nucleon struck by the pion and $\rho(0)$ is the matter density. This simple model gains support from the cross section ratios for inclusive pion scattering from the isotopic pair of ^{16,18}O nuclei.[11] This isospin dependence of the spreading potential reinforces the tendency of the Pauli effect in broadening the Δ^{++} more than in Δ^{-} in heavy nuclei.

A Δ spin-orbit potential of the form

$$\begin{aligned} &\Sigma_{\rm spr} = \Sigma^{C}_{\rm spr} + \Sigma^{LS}_{\rm spr} , \\ &\Sigma^{LS}_{\rm spr}(r) = V^{0}_{LS} \frac{1}{r} \frac{d\rho}{dr} 2\mathbf{L}_\Delta \cdot \boldsymbol{\Sigma}_\Delta \end{aligned} \tag{47}$$

was found to be necessary[2] in order to have a smooth energy dependence of $\Sigma_{\rm spr}$. We include this term in our optical potential as an L-dependent shift of the resonance denominator given by the doorway state expectation value

$$\Sigma^{L}_{LS} \equiv \langle D^{L}_{0}(k) \,|\, \Sigma^{LS}_{\rm spr} \,|\, D^{L}_{0}(k) \rangle \ , \tag{48}$$

where $|D^{L}_{0}(k)\rangle$ is the partial wave projection of Eq. (13). Specifically, we use the static-vertex form given in Ref. 3,

$$\Sigma^{L}_{LS} = -5 \frac{\langle \phi_L \,|\, \rho V^{0}_{LS} k^2 - (\rho V_{LS})' \frac{d}{dr} + \frac{L(L+1)}{2r} (\rho V_{LS})' \,|\, \phi_L \rangle}{\langle \phi_L \,|\, \rho k^2 - \rho' \frac{d}{dr} \,|\, \phi_L \rangle} \ , \tag{49}$$

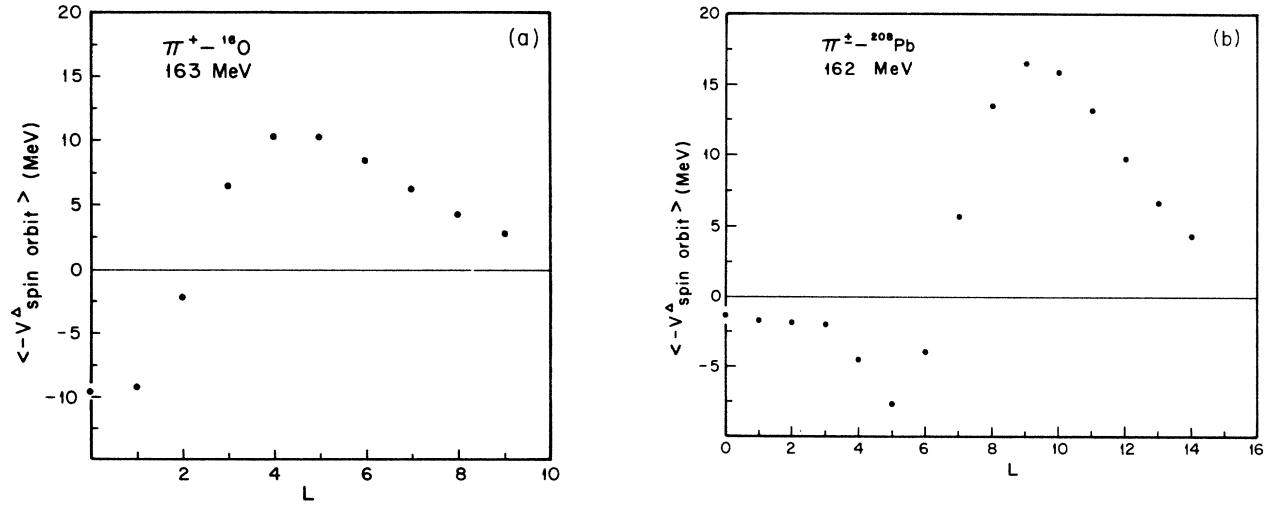

FIG. 2. The doorway expectation value of the negative of the Δ spin-orbit potential. (a) ^{16}O calculation at 163 MeV. (b) ^{208}Pb at 162 MeV.

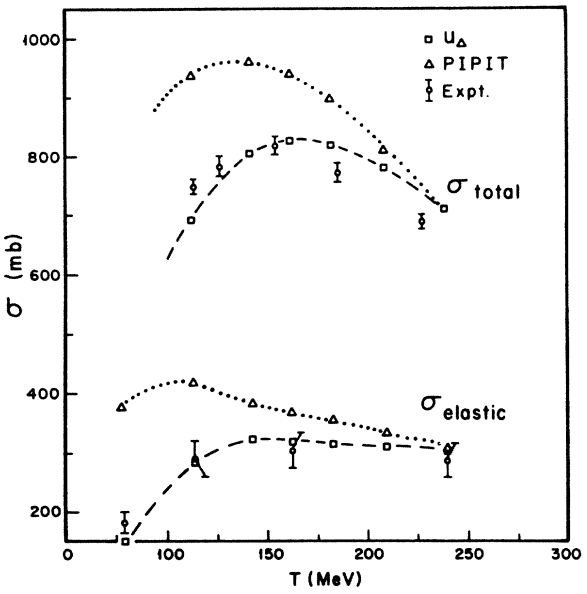

FIG. 3. π^+-^{16}O total and total elastic cross sections. Our work is shown by the dashed line and the PIPIT result by the dotted line. The data are from Refs. 16 and 17.

where ρ is the nuclear density and $\phi_L(r)=j_L(kr)$ is the free pion wave function with angular momentum L. The fit to the $\pi^{\pm}$-^{16}O elastic scattering angular distribution gave[2]

$$V_{LS}^0=(-10-4i)\ \text{MeV fm}^2\ . \tag{50}$$

The resulting L dependence is shown in Fig. 2. The spin-orbit term is repulsive for the central partial waves and attractive for the peripheral ones. Although it is not large in magnitude, the spin-orbit potential has an appreciable effect on the shapes of minima in the differential cross section.

III. APPLICATIONS

A. Pion-nucleus elastic scattering

The optical potential developed in the preceding section has been used to calculate pion elastic scattering from the closed shell nuclei ^{16}O and ^{208}Pb at pion energies ranging from 50 to 240 MeV, thus covering the energy region centered around the resonance. The results are compared both to Δ-hole calculations for ^{16}O and to a standard first-order optical potential calculation, namely PIPIT.[6] PIPIT is a momentum-space first-order optical potential code that uses a nonlocal, separable πN t matrix extended off-shell via the solution of the inverse scattering problem. The nuclear single particle densities and energies were systematically taken from the density-dependent Hartree-Fock results of Ref. 15.

1. π^+-^{16}O scattering

The study of π-^{16}O is particularly important since it allows us to establish contact with the available Δ-h calculations. The total and total elastic cross sections are shown in Fig. 3. The spreading potential reduces the

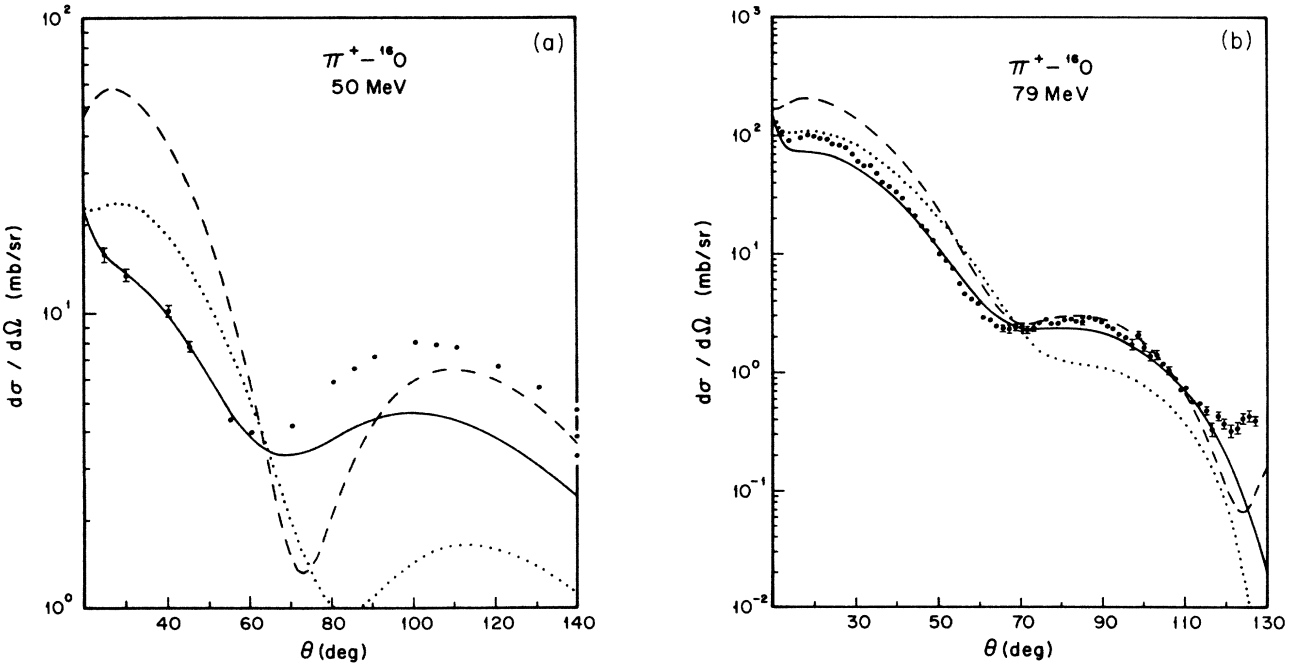

FIG. 4. π^+-^{16}O elastic differential cross sections at (a) 50, (b) 79, (c) 114, (d) 163, and (e) 240 MeV. Key: this work, solid line; PIPIT, dashed line; this work without an S-wave repulsive potential, dotted line. The data are from Ref. 17.

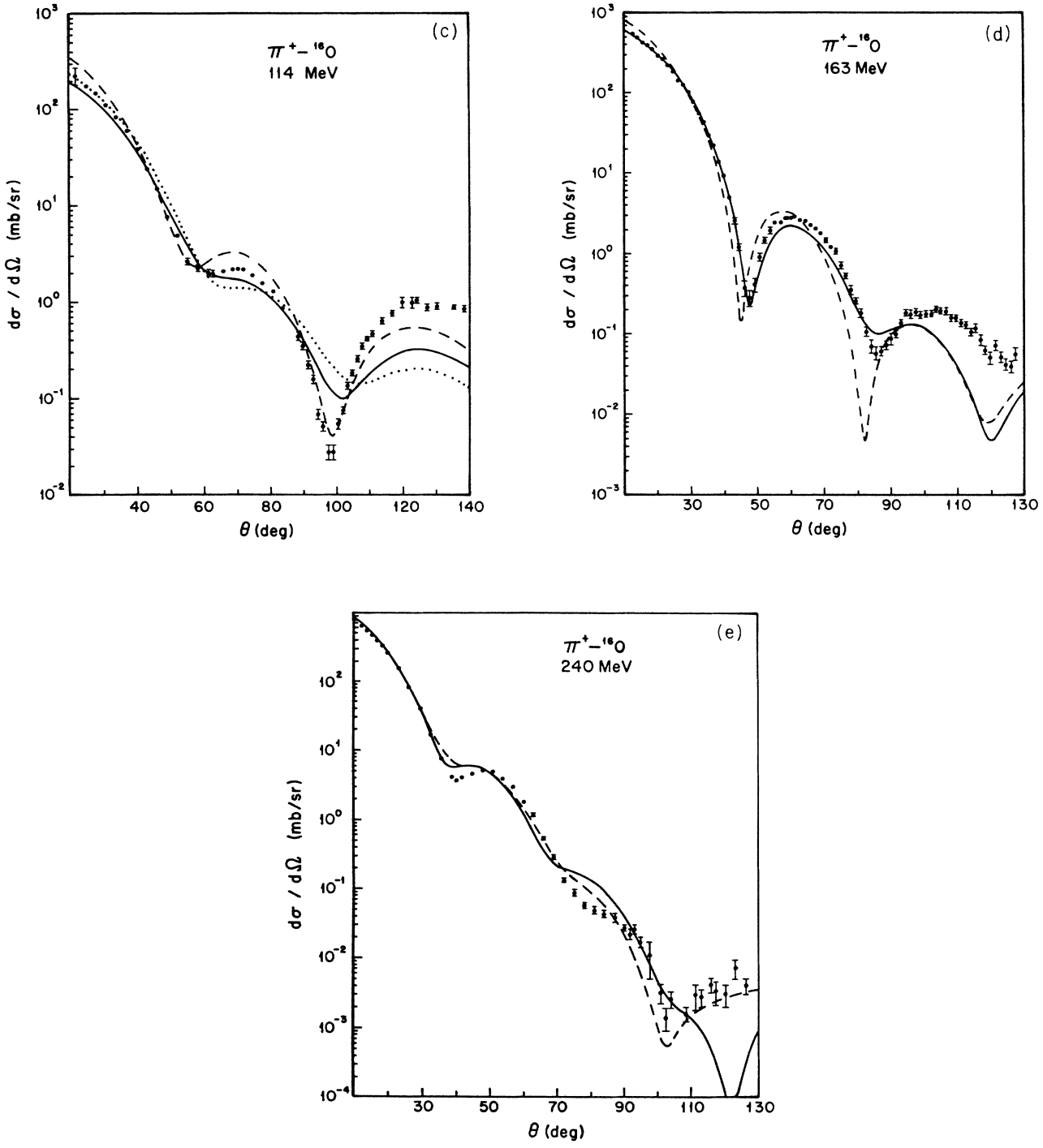

FIG. 4. (*Continued*).

cross section substantially from that predicted by the first-order optical potential PIPIT, in agreement with the data.[16] We stress that the strength of the central spreading potential, $(20-42i)$ MeV, is taken to be the same as that deduced in the Δ-hole calculations. The spreading potential reduces the resonant cross section by decreasing the optical potential strength [see Eq. (2)].

The elastic differential cross sections are shown in Fig. 4 for pion kinetic energies from 50 to 240 MeV. The data are from Ref. 17. The predictions are considerably better than are those of PIPIT. The forward cross sections are reproduced quite well and the location of diffraction structure is generally accurate. The phenomenological S-wave repulsion, Eq. (15) with $B_0=12$ MeV, plays an important role at the lower energies. The large angle cross sections are not reproduced well. This is also a systematic

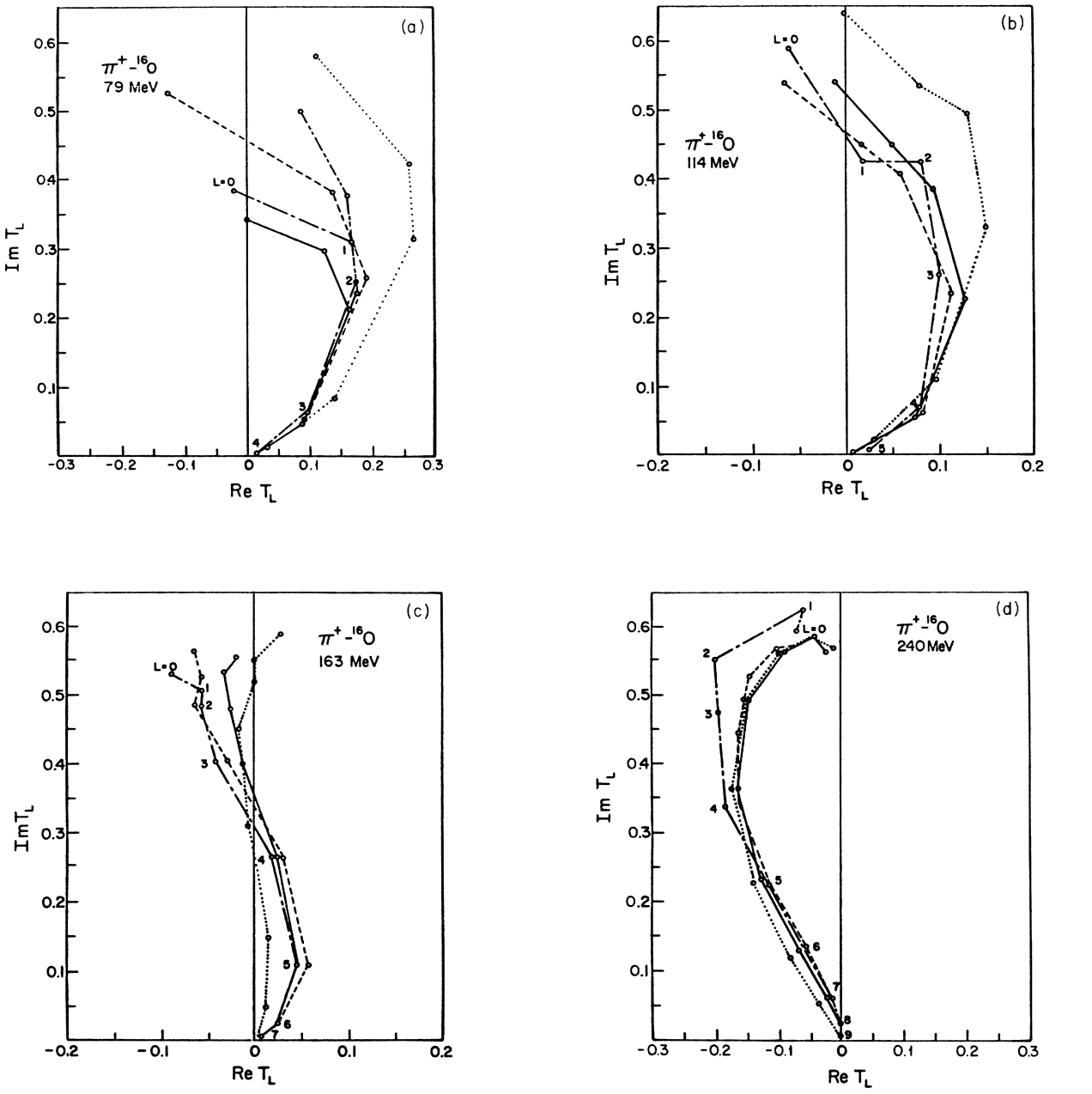

FIG. 5. Argand diagrams for π^+-^{16}O scattering at (a) 79, (b) 114, (c) 163, and (d) 240 MeV. Key: this work, solid line; Δ-h calculation of Ref. 1, dashed line; experimental fit of Ref. 1, dot-dashed line; PIPIT, dotted line; this work without S-wave potential, double dot-dashed line.

shortcoming of the Δ-hole calculations.

Although the comparison with data is satisfactory, comparison with the Δ-hole results[1] is important for establishing the validity of our approximations. We compare the partial wave amplitudes in the Argand plots of Fig. 5. The real and imaginary parts of the partial wave amplitudes

$$T_L \equiv \frac{\eta_L e^{2i\delta_L} - 1}{2i} \tag{51}$$

are shown as trajectories in L. We also show the partial wave amplitudes for PIPIT and for a phase shift fit to the data.[1] Clearly, our optical potential results are much closer to the Δ-hole and experimental results than to the PIPIT results. This is particularly true for the semiperipheral and peripheral partial waves, which are especially important for determining the cross section and are influenced primarily by the binding and propagation effects. The shortcomings of our approach appear in the central partial waves (e.g., recall the discussion of Pauli blocking).

Nevertheless, the results are clearly sufficiently encouraging to warrant further investigation.

Elastic $\pi^{\pm}$-^{208}Pb results are presented in Fig. 6 for two energies. The parameters used are identical to those employed in the ^{16}O calculations. The resonance calculations (including accurate wave functions) required about eight minutes and forty minutes of VAX 11/782 CPU time for the ^{16}O and ^{208}Pb cases, respectively. The data are from Ref. 18. Most of the observations made for the ^{16}O nucleus can be repeated here. The angular structure of the cross sections up to the second minimum and the forward elastic peak are well reproduced. It has not been necessary to adjust the c.m. collision energy or the nuclear density parameters unrealistically as has been done in applications of PIPIT in the literature. The same parameters of the isobar dynamics were used in π^- scattering and the agreement is as good as in the π^+ case, indicating the validity of the isospin dependence chosen for the medium corrections. The delta spin-orbit potential was found to have some effect at large angles.

The Argand plots for ^{208}Pb at resonance, Fig. 7, display a comparison between U_Δ and PIPIT results. The peripheral partial waves disagree substantially in the two calculations, indicating the failure of the static approximation. In the central partial waves, the complexity of the dynamics involved is indicated, but the dominance of strong absorption provides comparatively little leverage on the angular distributions. Nevertheless we can conclude that the optical potential based on Δ dynamics and using the same spreading potential as determined for ^{16}O provides a good description of scattering on ^{208}Pb.

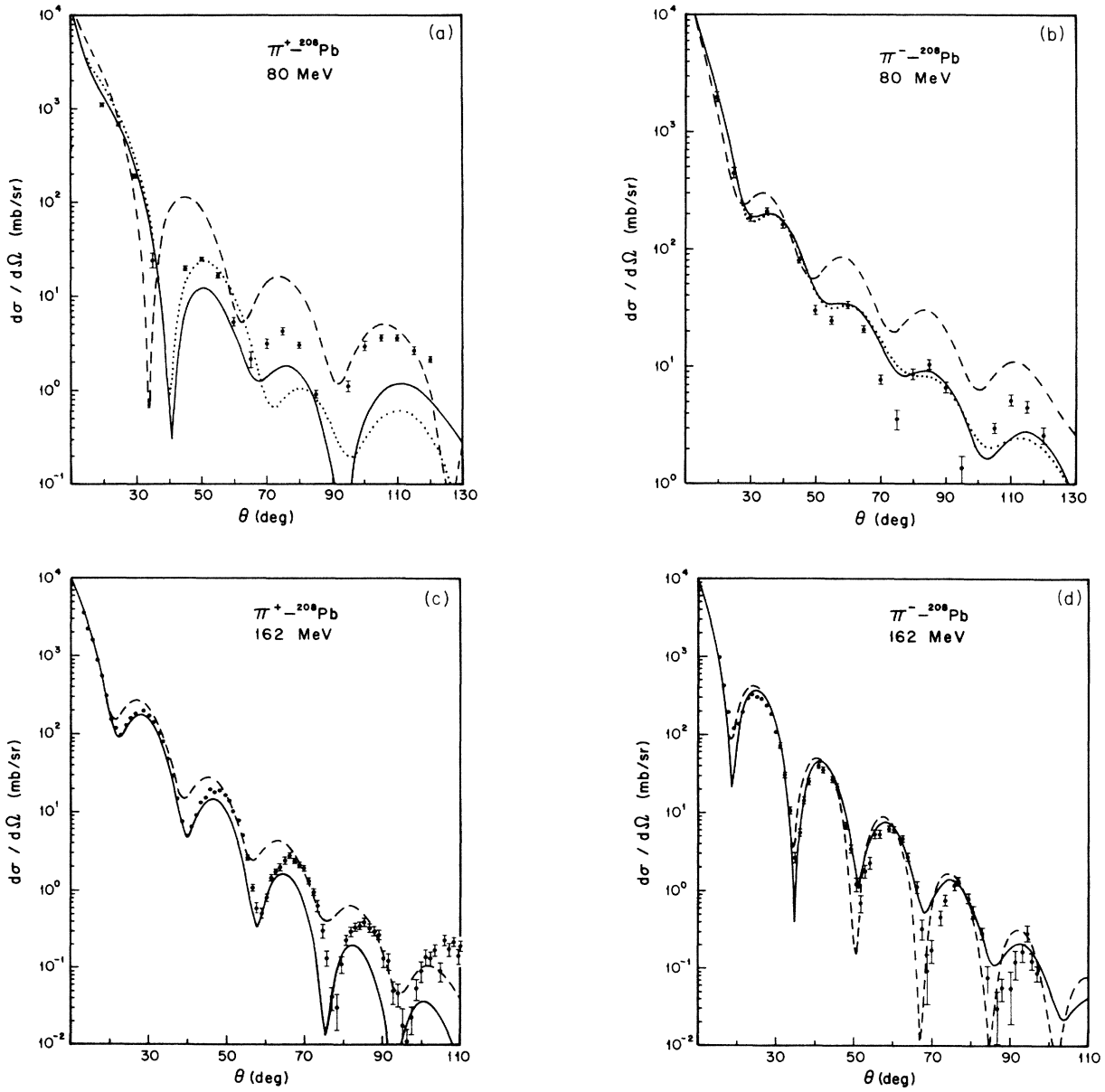

FIG. 6. $\pi^{\pm}$-^{208}Pb elastic differential cross section at 80 and 162 MeV. Key: this work, solid line; PIPIT, dashed line; this work without *S*-wave potential, dotted line. The data are from Ref. 18.

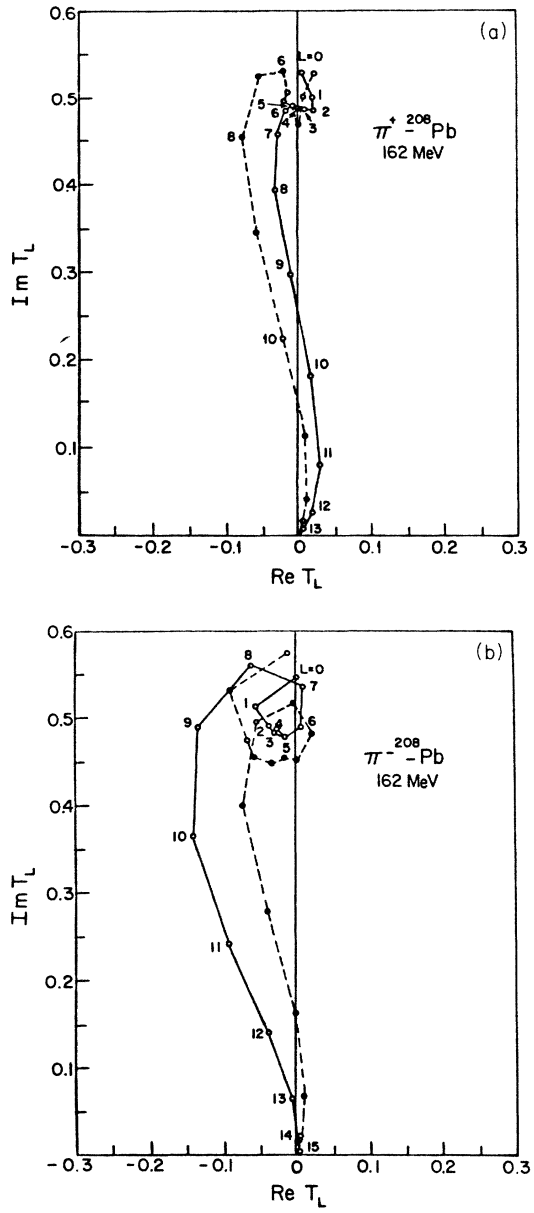

FIG. 7. Argand diagrams for pion ^{208}Pb scattering at 162 MeV. (a) π^+ scattering; (b) π^- scattering. Key: this work, solid line; PIPIT, dashed line.

B. Pion wave functions

In view of the applications to various pion-nucleus inelastic reactions, it is instructive to look at the pion wave functions as distorted by the optical potential. A convenient quantity to look at is the pion density at fixed impact parameter,

$$\rho^{(+)}(b,z) = |\psi_{k_0}^{(+)}(b,z)|^2 = \left|\sum_L (2L+1)U_L(k_0 r)P_L(\cos\theta)\right|^2 . \quad (52)$$

The incident probability density is normalized to unity and b is the impact parameter. Figure 8 displays $\rho^{(+)}$ for

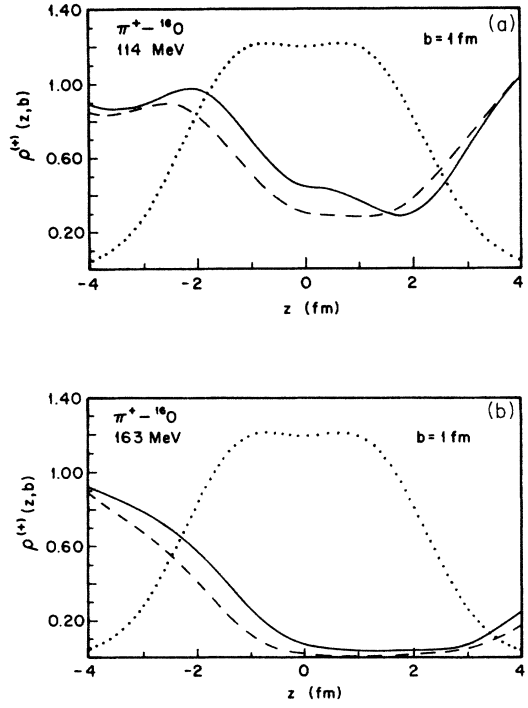

FIG. 8. Pion wave function in the ^{16}O nucleus at (a) 114 and (b) 163 MeV for an impact parameter $b = 1$ fm. Key: this work, solid line; PIPIT, dashed line; ^{16}O density profile, dotted line.

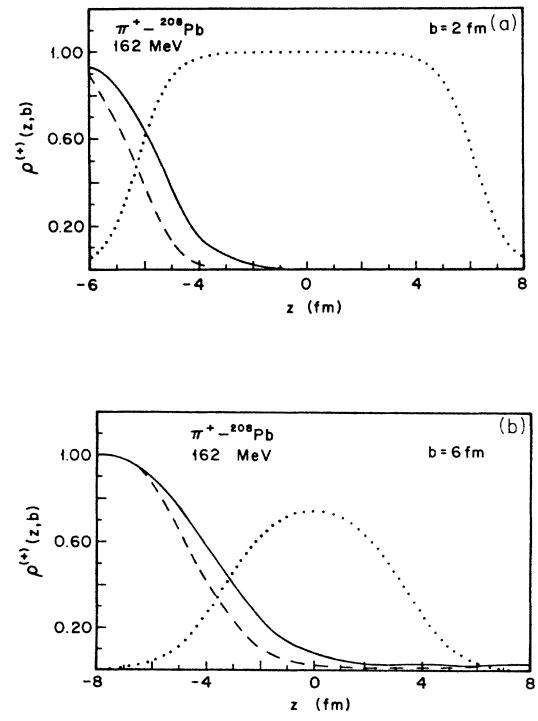

FIG. 9. π^+ density in ^{208}Pb nucleus at 162 MeV. Impact parameter $b = 2$ fm (a) and $b = 6$ fm (b). Key: this work, solid line; PIPIT, dashed line; ^{208}Pb density profile, dotted line.

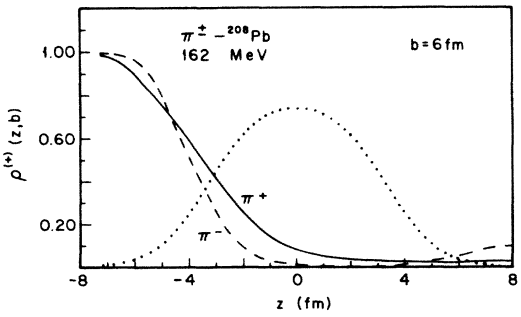

FIG. 10. Comparison of π^+ (solid line) and π^- (dashed line) densities in ^{208}Pb at 162 MeV and for $b=6$ fm. Dotted line: ^{208}Pb density profile.

an impact parameter $b=1$ fm at $T_\pi=114$ and 163 MeV in comparison with the PIPIT results. There is a sizable difference in the damping caused by the two optical potentials. Due to the combined effect of the spreading potential and the isobar propagation, the nuclear medium is less absorptive than the static theories predict. We also observe an interference effect on the back side of the nucleus (i.e., $z>0$), indicating that the eikonal approximation is not adequate. The optical potential is attractive below resonance and provides some focusing of the pions on the back side. For reference, the matter density of the target nucleus is also plotted at the appropriate impact parameter, where the matter density is normalized to unity at the origin $\mathbf{r}=(z,\mathbf{b})=0$ (note that the ^{16}O density is substantially larger than the central value at $b=1$ fm). Even near resonance, the pion wave function is found to penetrate rather deeply into the nucleus, particularly with the inclusion of Δ dynamics.

The π^+ densities near resonance are shown in Fig. 9 for ^{208}Pb for a central and for a peripheral impact parameter. The results are qualitatively similar to those seen in Fig. 8(b). The comparison of $\pi^\pm$ densities, shown in Fig. 10, has the expected behavior. The π^- density is enhanced relative to the π^+ well out in the surface region because of the Coulomb attraction. Inside the nucleus, the π^- density is more strongly damped because of the strong π^--neutron interaction.

C. Coherent π^0 photoproduction

The distorted pion wave functions are central ingredients in distorted wave calculations of inelastic processes. We present one simple application here, namely, coherent π^0 photoproduction through the Δ doorway. As has been discussed in considerable detail within the Δ-hole approach,[4] this reaction is a good one for demonstrating the importance of including Δ dynamics consistently in the transition operator as well as in the pion wave function.

We first give a brief derivation of the π^0-photoproduction cross section as used in this work. The coherent photoproduction amplitude in the isobar-hole picture is defined as

$$T_{\gamma\pi^0}=V_{P_0D}[D(E-H_\Delta)-W-\Sigma_{\rm Pauli}-\Sigma_{\rm spr}]^{-1}V_{D\gamma}\ , \quad (53)$$

where the γN-Δ vertex in the Δ rest frame is given by

$$V_{D\gamma}=g_\gamma\hat{\epsilon}(\mathbf{k},\lambda)\cdot\mathbf{k}\times\mathbf{S}T^0\ . \quad (54)$$

$\mathbf{k}$ is the photon momentum and $\hat{\epsilon}$ designates the photon polarization vector. The coupling constant g_γ is chosen to fit the experimental $M_{1+}(\frac{3}{2})$ multipole at resonance and has a value 0.165 fm. The other quantities were defined in Sec. II.

This expression is first written in a more conventional form, making the distortion operator explicit.[4] By expanding the denominator in terms of W and regrouping, we have

$$T_{\gamma\pi^0}=(1+T_{P_0P_0}G_{P_0})V_{P_0D}\times[D(E-H_\Delta)-\Sigma_{\rm Pauli}-\Sigma_{\rm spr}]^{-1}V_{D\gamma}\ , \quad (55)$$

$$T_{P_0P_0}=V_{P_0D}[D(E-H_\Delta)-W-\Sigma_{\rm spr}-\Sigma_{\rm Pauli}]^{-1}V_{DP_0}\ . \quad (56)$$

The first bracket in Eq. (55) generates the pion distorted waves. The remaining part is the production operator. Using the asymptotic plane waves for pion and photon, one writes

$$\langle\mathbf{q};0\,|\,T_{\gamma\pi^0}\,|\,\mathbf{k}\lambda;0\rangle'=\int\frac{d\mathbf{k}'}{(2\pi)^3}\langle\mathbf{q}\,|\,\Omega^{(-)\dagger}\,|\,\mathbf{k}'\rangle\langle\mathbf{k}';0\,|\,V_{P_0D}[D(E-H_\Delta)-\Sigma_{\rm Pauli}-\Sigma_{\rm spr}]^{-1}V_{D\gamma}\,|\,\mathbf{k}\lambda;0\rangle\ . \quad (57)$$

The differential cross section is obtained by averaging over the photon polarization directions

$$\frac{d\sigma}{d\Omega}=\tfrac{1}{2}\sum_{\lambda=\pm1}|\langle\mathbf{q};0\,|\,T_{\gamma\pi^0}\,|\,\mathbf{k}\lambda;0\rangle|^2\ . \quad (58)$$

One of the main ingredients of this calculation, namely the pion distorted wave, was examined in the last section. Here, we stress that, as seen from Eq. (55), the same medium corrections that were used in the distortion operator are also present in the production operator. A consistent treatment of both is important. This point is illustrated in Fig. 11, where the coherent π^0 photoproduction cross sections are calculated at various levels of approximation. The curve labeled IA (impulse approximation) has only plane waves and no medium corrections to the production operator. That labeled DW_0 is the standard DWIA result in which the pion wave function is distorted by an optical potential in which no medium corrections were included and the production operator remains unchanged. The curve labeled DW_1 includes the pion wave function distorted by the full optical potential with Δ dynamics but with the production operator still unchanged. Finally, the

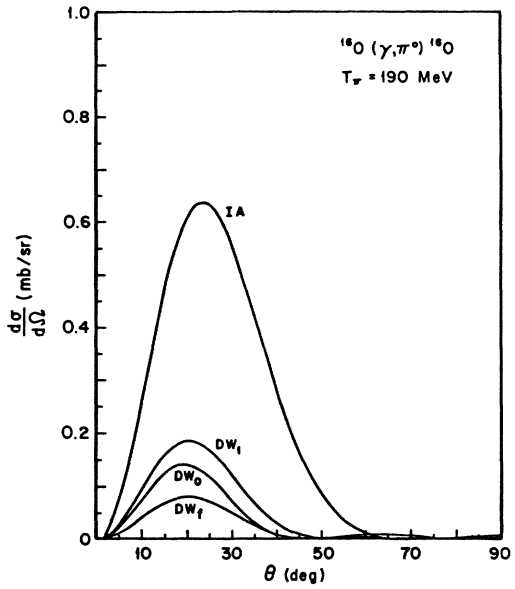

FIG. 11. Coherent π^0-photoproduction cross section in ^{16}O with pion kinetic energy 190 MeV. Labeling: impulse approximation (IA), distortion by a first-order optical potential (DW_0), distortion by the full optical potential (DW_1), and full distortion with medium corrections to the production operator (DW_f).

full calculation with both the distorted wave and the production operator including medium corrections is denoted DW_f. Naturally, the impulse approximation result (IA) is much larger than the others since the pion wave function is undamped. Near the resonance (190 MeV), the full optical potential leads to less attenuation of the pion wave function than does the first order static potential, and thus the DW_1 cross section is larger than the DW_0 one. However, this increase is compensated by the damping of the production operator near resonance due to medium corrections. Such effects have been discussed in the context of Δ-hole calculations and found to be important[4] in reproducing the available data on light nuclei.[19]

IV. CONCLUDING REMARKS

We constructed a pion optical potential which incorporates Δ dynamics. Our approach is basically that of the Δ-hole formalism as developed and applied in Refs. 1—4. That is, the "first order" effect of Δ propagation, binding, and Pauli blocking, all of which were found to be important in the Δ-hole studies, are incorporated "microscopically," while the "higher order" effect of pion annihilation is represented through a Δ spreading interaction. This phenomenology provides a rather different framework from that given by standard second order parametrizations. This is very evident from the enhanced pion density in the nucleus at resonance resulting from the inclusion of Δ dynamics.

We greatly simplified the problem by treating Δ propagation, Pauli blocking, and the nuclear density matrix in local density approximation. All of these approximations depend on the fact that the Δ propagates only a short distance before decay. We tested our model against the full Δ-hole calculations for π-^{16}O scattering and found good agreement, except in the most central partial waves. The application to $\pi^{\pm}$-^{208}Pb elastic scattering revealed good agreement with the data with the same mean field characterization of Δ-nucleus interactions as that extracted from the analyses of elastic scattering on light nuclei.

Freedman *et al.*[20] also constructed an optical potential based upon the earlier Δ-hole work. However, in the absence of a local density approximation for Δ propagation and for the nuclear density matrix, calculations with their optical potential retain much of the computational complexity involved in the full Δ-hole calculations. We have aimed explicitly at providing a flexible tool for application to a variety of reactions. Operationally, the code is a modified version of PIPIT,[6] with the resonant piece substantially changed and with an *S*-wave background potential added. The inputs for a calculation are just the proton and neutron distributions and the Δ-nucleus interaction parameters. Thus, in addition to providing a vehicle for studying the role of Δ dynamics, the optical potential developed here may be of broad use in the analysis of pion-nucleus data.

This work was supported in part through funds provided by the U.S. Department of Energy (DOE) under Contract No. DE-AC02-76ER03069.

[1]M. Hirata, F. Lenz, and K. Yazaki, Ann. Phys. (N.Y.) **108**, 116 (1977); M. Hirata, J. H. Koch, F. Lenz, and E. J. Moniz, *ibid.* **120**, 205 (1978).

[2]Y. Horikawa, M. Thies, and F. Lenz, Nucl. Phys. **A345**, 386 (1980).

[3]F. Lenz, M. Thies, and Y. Horikawa, Ann. Phys. (N.Y.) **140**, 266 (1982).

[4]J. H. Koch, E. J. Moniz, and N. Ohtsuka, Ann. Phys. (N.Y.) **154**, 99 (1984); J. H. Koch and E. J. Moniz, Phys. Rev. C **27**, 751 (1983).

[5]E. Oset and W. Weise, Nucl. Phys. **A319**, 365 (1979); T.-S. H. Lee and K. Ohta, Phys. Rev. C **25**, 3043 (1982).

[6]R. Eisenstein and F. Tabakin, Comput. Phys. Commun. **12**, 237 (1976).

[7]J. A. Carr, H. McManus, and K. Stricker-Bauer, Phys. Rev. C **25**, 952 (1982).

[8]See the papers of K. K. Seth and R. P. Redwine, in Proceedings of the International Conference on Particles and Nuclei, Heidelberg, 1984, edited by B. Povh and G. Z. Putlitz, Nucl. Phys. **A434**, 287c (1984) and **A434**, 239c (1984), respectively.

[9]T. Karapiperis and E. J. Moniz, Phys. Lett. **B148**, 253 (1984).

[10]G. S. Kyle *et al.*, Phys. Rev. Lett. **52**, 974 (1984).

[11]B. Karaoglu, T. Karapiperis, and E. J. Moniz, Phys. Rev. C **22**, 1806 (1980).

[12]L. S. Kisslinger and W. L. Wang, Ann. Phys. (N.Y.) **99**, 374 (1976).

[13]J. W. Negele and D. Vautherin, Phys. Rev. C **5**, 1472 (1972).
[14]E. J. Moniz and A. Sevgen, Phys. Rev. C **24**, 224 (1981).
[15]J. W. Negele, Phys. Rev. C **1**, 1260 (1970).
[16]A. S. Clough *et al.*, Nucl. Phys. **B76**, 15 (1974); N. D. Gabitzch *et al.*, Phys. Lett. **B47**, 234 (1973).
[17]J. P. Albanese *et al.*, Nucl. Phys. **A350**, 301 (1980); D. J. Marlbrough *et al.*, Phys. Rev. C **17**, 1395 (1978).
[18]C. Olmer *et al.*, Phys. Rev. C **21**, 254 (1980); M. J. Leitch *et al.*, *ibid.* **29**, 561 (1984).
[19]D. R. Tieger *et al.*, Phys. Rev. Lett. **53**, 755 (1984).
[20]R. A. Freedman, G. A. Miller, and E. M. Henley, Phys. Lett. **B103**, 397 (1981).